RSC Advances

ROYAL SOCIETY OF CHEMISTRY

www.rsc.org/advances

Fabrication and performance study of zwitterionic polyimide antifouling ultrafiltration membrane

Yang Liu, Chao Ma, Shaofeng Wang, Hanxiang Guo, Binhan Zhang, Li Zhang, Kaili Gu, Jiyou Gu*

College of Material Science and Engineering, Northeast Forestry University, Harbin 150040, PR China

*Corresponding author. Tel.: +86 451 8219 0635; fax: +86 451 8219 0635.

E–mail address: dldgujy@nefu.edu.cn (J. Gu)

Abstract:

In this paper, the new aromatic zwitterionic polyimide (PI) copolymer was synthesized by a one-pot polymerization reaction and used to prepare the fouling-resistant ultrafiltration membrane. The obtained polymer was thoroughly characterized by differential scanning calorimetry (DSC) and thermogravimetric analysis (TGA) and exhibited excellent thermal stability. Meanwhile, the zwitterionic PI membrane was compared to the reference PI membrane to determine changes in hydrophilicity, performance and antifouling property. The results displayed that the surface hydrophilicity, pure water flux and protein solution permeation of the zwitterionic PI membrane was remarkably higher than those of the reference PI membrane. The cycle ultrafiltration experiment for protein solution revealed that nonspecific protein adsorption, especially irreversible protein adsorption, for the zwitterionic PI membrane was significantly reduced, suggesting superior antifouling performance. In sum, the zwitterionic PI is employed as the polymer-based membrane material, resulting in the ultrafiltration membrane with long-term performance stability.

Keywords: Zwitterionic, Polyimide, Ultrafiltration, Antifouling

1. Introduction

Every year, the 15% of the energy produced worldwide is employed for various separation processes, but most of them are inefficient.[1] Fortunately, among these separation technologies available today, membrane technology, especially ultrafiltration (UF), is regarded as the most economical and effective separation process since it involves a number of attractive features including low energy consumption, mild operating conditions, no additive requirements, no phase change and environmentally friendly.[2] Ultrafiltration is mainly used for processing macromolecules such as suspended colloids, proteins, polysaccharides and nucleic acids, while passing water and low molecular weight solutes, which has achieved unprecedented success on a global scale and played an important strategic role in many industrial processes mainly environmental control, wastewater treatment, nanotechnology, pharmacy, biotechnology, and chemical industry, etc.[3] There is no doubt that ultrafiltration will expand rapidly into many conventional and new applications in the future. However, membrane fouling is a major obstacle to the widespread deployment of ultrafiltration technology. It is a process where solute or particles adsorb on the membrane surface or adhere to the membrane pores in a way that degrades the membrane performance.[4] Membrane fouling can cause severe flux decline and affect the water production capacity, and alter membrane selectively. In addition, severe fouling may shorten membrane life and require intense chemical cleaning or membrane replacement, which increases the operating costs of the treatment plant.[5,6] Even though membrane fouling is an inevitable phenomenon, it can be minimized by several strategies, such as an adequate pretreatment, a reasonable selection and design of the membrane module, and the introduction of effective membrane cleaning measure, etc.[7] It is well known that membrane material is the central or most important part of separation membrane. Therefore, more and more researches have reported reduction of membrane fouling by the straightforward synthesis and/or modification of the membrane material,[8-12] especially the direct development of the zwitterionic polymer membrane material.[13,14]

Zwitterionic polymers, containing typically the same number of anionic and cationic groups in the polymer chain, are promising alternative membrane materials with an excellent antifouling ability.[15] Despite a high density of ion pairs attached to the polymer chain, the overall charge of zwitterionic polymers is zero under normal conditions.[14] Up to now, numerous significant works

have been made in preparing high performance zwitterionic polymer membranes that were shown to reduce protein adsorption, because their hydrophilic surfaces containing uniform chains with tailorable length could bind a large amount of water to form the hydration layer as a physical and energy barrier, leading to a strong repulsive force to protein at specific separation distances or making the protein contact with the surface without conformation change.[16,17] For instance, Shi et al. first prepared a kind of zwitterionic tertiary amine-modified polyethersulfone (TA-PES) as membrane material that displayed superior anti-protein-fouling property and excellent untraliltration performance.[18] In another study, Zhang et al. developed a novel zwitterionic carboxybetaine poly(arylene ether sulfone) (PES-CB) material, and the water flux recovery ratio as high as 95% was achieved for the PES-CB membrane after three cycles of lysozyme solution filtration.[19] Moreover, Su and coworkers synthesized two kinds of poly(acrylonitrile)-based zwitterionic copolymers PAN-DMMSA and PAN-MPDSAH, both can be used for preparation of efficient and reusable ultrafiltration membranes.[20,21]

Polyimides (PIs) are one of the most favorable candidates for the separation membrane due to their excellent heat resistance, chemical stability, mechanical strength and good film-forming ability.[22] Owing to the multiple possible synthetic approaches, PI can be prepared with an accurate molecular design and functionalized with respect to the applicative purposes. A variety of PIs on various available monomers provides a good opportunity to better understand the structure-property (or performance) relationships of ultrafiltration membranes. It was expected that the zwitterionic PI membrane provide a good opportunity to improve antifouling property. With this perspective, the present study reports on the synthesis of novel aromatic zwitterionic PI copolymer that was used in the preparation of antifouling ultrafiltration membrane by phase inversion method. The chemical structure and thermal properties of the zwitterionic PI copolymer were thoroughly characterized with Fourier transform infrared spectrometry (FTIR), ^{1}H NMR spectroscopy, differential scanning calorimetry (DSC) and thermogravimetric analysis (TGA). In addition, the morphology and surface hydrophilicity of the zwitterionic PI membranes were studied with scanning electron microscopy (SEM) and water contact angle measurements. The membrane performance was evaluated during bovine serum albumin (BSA) cycle ultrafiltration experiments and the antifouling performance of the zwitterionic PI membrane was examined. Meanwhile, the PI membrane without zwitterionic group was used as a benchmark reference for

evaluating the membrane performance, and a detailed performance comparison has been made.

2. Experimental

2.1 Chemicals and materials

N,*N*-dimethyl-*p*-phenylenediamine and 2,5-dihydroxybenzenesulfonic acid potassium salt were purchased from Alfa Aesar and used without further purification. 4-Nitrofluorobenzene, palladium/activated carbon (Pd/C), cesium fluoride (CsF), anhydrous potassium carbonate (K_2CO_3), hydrazine monohydrate, *m*-cresol, trimethylamine (TEA), benzoic acid, isoquinoline were purchased from Aladdin Reagent, China. 4,4′-diaminodiphenyl ether (ODA) was used as received from Tokyo Chemical Industry (TCI), Japan. 4,4′-Oxydiphthalic dianhydride (ODPA) (TCI) was purified by recrystallization from acetic anhydride. Poly(vinylpyrrolidone) (PVP 30 K), which was used as pore-former, was purchased from Fluka Chemika, Switzerland. Bovine serum albumin (BSA, pI=4.8, M_w=67,000) and phosphate buffer solution (PBS, 0.1 mol/L, pH 7.4) were both purchased from Dingguo Bio-technology Co., Ltd. (Beijing, China). Coomassie brilliant blue G250 was purchased from Aldrich. Dimethyl sulfoxide (DMSO) and *N*,*N*-dimethylformamide (DMF) were purified by distillation under reduced pressure over calcium hydride prior to use and stored over molecular sieves. *N*-methyl-2-pyrrolidinone (NMP), toluene, ethanol and methanol were supplied by Beijing Chemical Reagent, China. All other reagents were used as received from commercial sources and used without further purification. Deionized water was used throughout this study.

2.2 Synthesis of diamine monomers

2.2.1 Synthesis of 4,4′-diamino-4″-(dimethylamino)triphenylamine (TPA-NMe_2)

4,4′-diamino-4″-(dimethylamino)triphenylamine (TPA-NMe_2) was obtained in a two-step manner according to previously reported procedure,[23] and the synthetic route is outlined in Scheme 1. First of all, 4,4′-dinitro-4″-(dimethylamino)triphenylamine was prepared through a characteristic nucleophilic displacement reaction by treatment of 4-nitrofluorobenzene with *N*,*N*-dimethyl-*p*-phenylenediamine in dried DMSO in the presence of dried cesium fluoride. In the second step, the target diamine monomer was obtained by hydrazine Pd/C-catalyzed reduction of the intermediate dinitro compound.

2.2.2 Synthesis of 2,5-bis(4′-aminophenoxy)benzenesulfonic acid potassium salt (BAPBS)

As shown in Scheme 2, 2,5-bis(4′-aminophenoxy)benzenesulfonic acid potassium salt (BAPBS) was synthesized in a two-step procedure. In the first step, a mixture of 22.83 g (0.1 mol) of 2,5-dihydroxybenzenesulfonic acid potassium salt, 31.04 g (0.22 mol) of 4-nitrofluorobenzene, 16.58 g (0.12 mol) of anhydrous potassium carbonate, 150 mL of dry DMF, and 50 mL of toluene was placed in a 500-mL, three-necked, round-bottomed flask equipped with a mechanical stirrer, a Dean-Stark trap, a reflux condenser and a nitrogen purge. The mixture was refluxed with stirring at 130 ºC for 4 h to dehydrate the system. After removal of toluene, the reaction temperature was increased to 150 ºC and maintained at this temperature for another 8 h. Once the reaction was complete, the solution was cooled below 80 ºC and then poured into cold water. A solid precipitate was filtered off, washed with water and ethanol successively, and dried under vacuum. Then 39.44 g of yellow product was obtained (83.8%).

In the second step, a total of 14.11 g (0.03 mol) of the previously obtained intermediate dinitro monomer, 0.25 g of 10% Pd/C, and 120 mL of ethanol were mixed in a 250-mL, three-necked, round-bottomed flask equipped with a mechanical stirrer and a reflux condenser. Subsequently, under a nitrogen atmosphere, 15 mL of hydrazine monohydrate was added slowly to the mixture at the reflux temperature. After a further 8 h of reflux, the reaction solution was filtered under hot state to remove Pd/C catalyst, and the filtrate was cooled under nitrogen atmosphere to precipitate slight yellow crystals. The crude product was filtered and dried. The pure product was obtained by recrystallization from a mixture of ethanol and water to afford 8.16 g (yield: 66.3%) of white crystals.

2.3 Synthesis of zwitterionic and reference PI copolymers

The aromatic zwitterionic PI random copolymer was synthesized with TPA-NMe_2, BAPBS, ODA and ODPA by a conventional two-step method via chemical imidization reaction, and the synthetic route is illustrated in Fig. 1. The typical procedure was as follows. To a 100 mL three-neck flask were added 0.4776 g (1.5 mmol) of TPA-NMe_2, 0.6157 g (1.5 mmol) of BAPBS, 1.4017 g (7.0 mmol) of ODA, 1.2143 g (12.00 mmol) of triethylamine and 49 mL of *m*-cresol under nitrogen flow with stirring at room temperature. After obtaining a clear homogeneous solution, 3.1021 g (10.0 mmol) of ODPA and 1.7097 g (14.0 mmol) of benzoic acid were added. The solid content of the solution is approximately 10 wt%. The mixture was stirred at room temperature for a few minutes and then heated at 60 °C for 4 h and 180 °C for 20 h. Water formed

during the imidization was continuously removed with a stream of nitrogen. After cooling to 80 °C, an additional 20 mL of *m*-cresol was added to dilute the highly viscous solution, which was then poured into a large excess of methanol under vigorous stirring. The green fiber-like precipitate was filtered off, washed with methanol thoroughly, and dried in vacuum, giving the target product with a yield of 95.4%.

In this work, the reference PI was synthesized with ODA and ODPA, which was used as a benchmark reference for evaluating the membrane performance because its chemical structure similarity to the zwitterionic PI. The reference PI was prepared as follows: the diamine (ODA, 2.0024 g, 10.0 mmol) and dianhydride (ODPA, 3.1021 g, 10.0 mmol) were dissolved together in *m*-cresol with isoquinoline (2.5 mL) as a catalyst. The reaction mixture was gently heated to 60 °C under stirring for 4 h, followed 180 °C for 20 h. After cooling to 80 °C, an additional 20 mL of *m*-cresol was added to dilute the highly viscous solution, which was then poured into a large excess of methanol under vigorous stirring. The white fiber-like precipitate was filtered, then washed with methanol, and dried under vacuum, giving the target product with a yield of 96.8%.

2.4 Membrane preparation

The zwitterionic PI membrane was prepared by the conventional immersion precipitation phase inversion method. The zwitterionic PI was dried at 80 °C under vacuum for at least 24 h before use. Homogeneous casting solution was prepared by dissolving the zwitterionic PI and PVP in NMP at 50 °C under vacuum and filtered by a metal filter. The concentrations of the zwitterionic PI and PVP in the casting solution were 15 wt.% and 5 wt.%, respectively. After degassing, the solution was cast onto a polyester nonwoven fabric supported by a glass plate using a casting knife with a nominal thickness of 200 μm, and then the glass plate was immersed immediately into a coagulating bath of deionized water at room temperature (about 22 °C). Finally, the membrane was kept in deionized water for at least 48 h until all of solvent and water-soluble polymer were removed. The salt-form PI membrane was immersed in a 1M H_2SO_4 at room temperature for 24 h to convert it to the zwitterionic form by proton exchange. The reference PI membrane was prepared by the same procedure as the zwitterionic PI membrane.

2.5 Characterization

2.5.1 Monomer and polymer characterization

The experimental details and results of the monomer and polymer characterizations are given in

supplementary information.

2.5.2 Membrane characterization

The characteristics of the membranes were investigated using the following parameters: morphology, contact angle, porosity and pore size. The membranes used for characterization were dried under vacuum at 50 ºC for 24 h.

The surface and cross-section morphologies of the membranes were examined by a scanning electron microscope (SSX-550, Shimadzu equipped with energy dispersive X-ray (EDX) spectroscopy device). The membranes were frozen in liquid nitrogen and fractured to avoid destroying the structures, and sputtered with gold prior to SEM observation.

The static water contact angles of the membranes were estimated by sessile drop method with a contact angle goniometer from Drop Shape Analysis (DSA 100 KRUSS GMBH, Hamburg) at room temperature. About 4 μL of deionized water was dropped onto the membrane surface with a microsyringe, and the value of water contact angle was recorded after 3 s. At least five measurements in different locations of the membrane samples were carried out and averaged to yield the contact angles. In addition, the surface free energy was also calculated according to the following equation:

$$\cos\theta = -1 + 2\sqrt{\frac{\gamma_s}{\gamma_l}}e^{-\beta(\gamma_s-\gamma_l)^2} \qquad (1)$$

where γ_s and γ_l represent the solid and liquid surface free energy, respectively. θ is the contact angle of the membrane sample. The value of water surface free energy is 72.8 mJ/m^2. β is the constant coefficient related to a specific solid surface and the value of 0.0001247 is adopted from previously reported literature.[24]

The porosity of the membranes were measured by the dry-wet weight method which was calculated according to Eq. (2):[25]

$$\varepsilon = \frac{m_1 - m_2}{\rho_w A l} \qquad (2)$$

where ε is the porosity (%), m_1 is the weight of the wet membrane (g), m_2 is the weight of the dry membrane (g), ρ_w is the water density (0.998 g/m^2), A is the effective area of the membrane (cm^2), and l is the membrane thickness (μm).

Average pore size r_m (m) was determined by the filtration velocity method according to the

Guerout-Elford-Ferry equation, which can be calculated as follow:[26]

$$r_m = \sqrt{\frac{(2.9-1.75\varepsilon)\times 8\eta l Q_t}{\varepsilon \times A \times \Delta P}} \qquad (3)$$

where Q_t is the volume of the permeate water per unit time (m^3/s), ΔP is the operational pressure (0.1 MPa), and η is the viscosity of water (8.9×10^{-4} Pa.s) at 25 ºC. In order to minimize experimental error, each membrane was measured for three times and calculated the average.

2.6 Protein adsorption experiments

The amount of proteins adsorbed on membrane is one of the most important evidence in evaluating the fouling resistant ability of membranes, and BSA was used as model protein to evaluate the anti-protein adsorption performance of two investigated membranes in phosphate buffered saline (PBS, pH 7.4). The membrane samples were cut into a round shape with a diameter of about 30 mm, and treated by ultrasonication for 30 min in 0.1 M PBS solution for cleanness. Then the pre-treated membranes were immersed into PBS solution containing BSA (1.0 mg/mL) at 25 ºC for 4 h. After adsorption, each membrane was rinsed three times in the fresh PBS by gentle shaking. Then these membranes were transferred into a well-plate filled with PBS solution, and the protein adsorbed on the membrane surface was completely desorbed by ultrasonic treatment at room temperature for 3 min. The obtained PBS solution was dyed with Coomassie Brilliant Blue and measured by a UV-vis spectrophotometer (UV3600, Shimadzu) to determine the total amount of adsorbed protein. The final results were averaged from triplicate specimens for each membrane.

2.7 Ultrafiltration experiments

The membrane performances were tested using a stirred dead-end filtration cell at room temperature, and the effective membrane area is around 12.6 cm^2. At first, each membrane was initially subjected to pure water with pressure of 0.2 MPa for 1 h prior to performing the ultrafiltration experiments. Then the pressure was lowered to 0.1 MPa and all the ultrafiltration experiments were carried out at this pressure. After compacted, deionized water was passed through the membrane for 1 h to obtain the beginning pure water flux ($J_{w,0}$, L/m^2h), and the flux was measured every 5 min. In this present study, three cycles of filtration experiment was carried out for each membrane sample. In each cycle, a BSA solution with a concentration of 1.0 mg/mL in PBS (pH 7.4) was filtrated for 2 h. The flux during protein filtration was recorded. After BSA

solution filtration, the membrane was washed thoroughly and passed through deionized water for another 30 min (the washing time was not counted in the filtration cycle). Thereafter, the pure water flux was measured again within 1 h for the membrane, which was recorded as $J_{w,i}$. The flux (J_w and J_p) of the membrane was determined by direct measurement of permeate volume, which was calculated following the equation:

$$J = \frac{V}{At} \qquad (4)$$

where V was the volume of permeation, A was the effective membrane area and t was the permeation time. In order to evaluate the recycling property of these membranes, the flux recovery ratio (FRR_i) during the ith cycle is calculated using the following expression:

$$FRR_i(\%) = \left(\frac{J_{w,i}}{J_{w,i-1}}\right) \times 100 \qquad (5)$$

The higher FRR value, the better the antifouling property of the membrane. The membrane rejection ratio (R) was calculated using the following equation:

$$R(\%) = \left(1 - \frac{C_p}{C_f}\right) \times 100 \qquad (6)$$

In which C_p (mg/L) is the permeate concentration and C_f (mg/L) is the feed concentration. The solute concentration of permeation was measured by a UV-vis spectrophotometer (UV3600, Shimadzu).

To study the antifouling property in more detail for the zwitterionic and reference PI membranes, the degree of total flux loss caused by total protein fouling in the ith cycle, $R_{t,i}$, was defined as

$$R_{t,i}(\%) = \left(\frac{J_{w,i-1} - J_{p,i}}{J_{w,i-1}}\right) \times 100 \qquad (7)$$

A high value of $R_{t,i}$ corresponds to a large flux decay and serious membrane fouling. The total flux loss was caused by both reversible and irreversible protein fouling in the ith cycle. $R_{r,i}$ was calculated following the equation:

$$R_{r,i}(\%) = \left(\frac{J_{w,i} - J_{p,i}}{J_{w,i-1}}\right) \times 100 \qquad (8)$$

which was the reversible fouling ratio caused by reversible fouling, and could be eliminated by

hydraulic cleaning. And $R_{ir,i}$ was calculated following the equation:

$$R_{ir,i}(\%) = \left(\frac{J_{w,i-1} - J_{w,i}}{J_{w,i-1}} \right) \times 100 = R_{t,i} - R_{r,i} \qquad (9)$$

which was the irreversible fouling ratio caused by irreversible fouling, and can only be eliminated by chemical cleaning or enzymatic degradation.[27,28] $R_{t,i}$ was the sum of $R_{r,i}$ and $R_{ir,i}$.

3. Results and discussion

3.1 Membrane Characterization

The scanning electron microscopy (SEM) was employed to investigate the differences in the surface morphology of the zwitterionic and reference PI membranes (Fig. 2). It is apparent that two investigated membranes have typical asymmetric structures, which consist of the thin dense skin layer and the porous sublayer. However, the introduction of the zwitterionic group results in some microstructure changes as revealed in the cross-sectional SEM images (Fig. 2(a)). The reference PI membrane has a long and thin finger-like structure while the finger-like macrovoids in the zwitterionic PI membrane become wider. The sulfonic acid groups make a big increase in the hydrophilicity, which possibly greatly interferes with the phase inversion process for membrane formation. This phenomenon is comparable with the sulfonated ultrafiltration membrane previously reported in the literature.[9] In general, a highly porous sublayer with many finger-like macrovoids and a finely porous, thin skin layer are formed when the precipitation process is fast due to instantaneous liquid–liquid dimixing process, whereas the slow precipitation (the delayed liquid–liquid dimixing process) results in a porous sublayer (often with fewer macrovoids) with a dense, relatively thick skin layer.[29] The result indicates that the introduction of the sulfonic acid and tertiary amine groups can result from the delayed phase separation, as the zwitterionic PI precipitates slowly and thus creates larger finger-like macrovoids. Another obvious difference between these membranes is in their top surface morphologies. The reference PI membrane showed a relatively smooth surface, and the surface of the zwitterionic PI membrane became much rougher. It can be explained that the zwitterionic PI membrane contains many polar sulfonic acid groups, which means higher water uptake, and thereby the surface of the zwitterionic PI membrane is excessively swollen. Furthermore, the energy-dispersive X-ray (EDX) S mapping on the surfaces of the zwitterionic and reference PI membranes is also shown in Fig. 2. It could be

seen that elemental sulphur (the blue bright spots) is evenly distributed on the zwitterionic PI membrane surface. In contrast, there is no elemental S on the surface of the reference PI membrane. Since the sulfonic acid group is the only source of elemental S, EDX measurement gave valuable information to confirm that the zwitterionic PI was successfully synthesized.

Surface hydrophilicity is one of the most important factors in determining antifouling property and performance of the ultrafiltration membrane. The hydrophilicity and wettability of the zwitterionic and reference PI membranes in this study was evaluated by contact angle measurement, which was also used to assess the surface (interfacial) free energies of substrate surfaces. It is commonly accepted that the lower contact angle represents the greater tendency for water to wet the membrane, the higher surface energy and the higher hydrophilicity. Table 1 lists the detailed water contact angle and surface energy data from the measurements on these different membranes, which clearly reveals the changes in the hydrophilicity of the zwitterionic and reference PI membrane. The reference PI membrane has the higher contact angle of 81.7º (Fig. 3(a)), indicating lower hydrophilicity. Comparing with the reference PI membrane, a significant decrease of water contact angle (63.2º) and an increase of the surface energy (45.8 mJ/m^2) were observed for the zwitterionic PI membrane in Fig. 3(b). This tendency was attributed to the hydrophilic nature of the sulfonic acid groups. The zwitterionic groups can form a hydration layer via electrostatic interaction in addition to the hydrogen bond.[17,30] Therefore, the introduction of the sulfonic acid and tertiary amine groups can effectively enhance hydrophilicity and improve antifouling property of ultrafiltration membranes.

3.2 Membrane performance

3.2.1 Protein adsorption of the zwitterionic and reference PI membranes

The static protein adsorption is one of the dominant factors determining the membrane fouling property. Herein, BSA was used as the model protein to evaluate the static protein adsorption on the surface of the zwitterionic and reference PI membranes. The antifouling property of membrane is highly dependent on the membrane surface chemistry, such as surface charge character, free energy, chemical composition and morphology. In many cases, a nonspecific protein adsorption on a hydrophobic membrane surface can cause a serious membrane fouling. Therefore, the increment in the surface hydrophilicity is a straightforward and effective method to enhance the antifouling property of a membrane.

As is shown in Fig. 4, the reference PI membrane displays a higher protein adsorption due to its hydrophobic character, and the zwitterionic PI membrane exhibits a lower adsorption, which can be attributed to the introduction of the hydrophilic sulfonic acid groups. Interestingly, this order is very similar to the trend found in the static water contact angle measurement. In general, the protein resistant chemical structures are commonly hydrophilic, overall electrically neutral, hydrogen-bond acceptors but not hydrogen-bond donors,[31] and the polymer applied in this work shares all of these common characteristics. It is commonly believed that zwitterions form a regular hydration layer via electrostatic interactions in addition to hydrogen bond, and the protein was excluded from the hydration layer to avoid the entropy loss caused by the entrance of large protein molecules into the highly structural layer.[32] Our study indicated that the zwitterionic PI membrane exhibit an effectively reduced protein adsorption and show prominent antifouling properties. The experimental results were consistent with the general antifouling mechanism for zwitterionic membranes.[5,17]

3.2.2 Permeation properties of the zwitterionic and reference PI membranes

Ultrafiltration experiments were carried out to investigate the separation performance of the zwitterionic and reference PI membranes. Fig. 5 presents time-dependent flux during ultrafiltration operation, which shows that the flux of the membrane can be improved with the introduction of the zwitterionic groups. The zwitterionic PI membrane always kept much higher flux for both water and BSA solution than the reference PI membrane, which can be attributed to the increased hydrophilicity and surface morphology change of the zwitterionic PI membrane. Moreover, this result could be proved quantitatively by determining the average pore size. The average pore sizes of the two investigated membranes were calculated by Eq. (3). In this study, the zwitterionic PI membrane has the higher average pore size (13.7 nm), comparing to that of the reference PI membrane (10.3 nm), which is in accordance with above discussion on the water flux measurements.

As shown in Fig. 5, the flux decreased dramatically at the first ultrafiltration of BSA solution due to membrane fouling caused by protein adsorption or deposition on the membrane surface. When the adsorption and deposition of protein molecules approached equilibrium, a relatively steady flux (J_p) was retained. The BSA rejection ratio (R) of the reference PI membrane is 99.5%, and that of the zwitterionic PI membrane is 95.4%. Therefore, the smaller pore size of the

reference PI membrane had a positive effect on BSA rejection.

After 2 h of the filtration of BSA solution, the membranes were washed thoroughly and passed through deionized water for another 30 min, and the water fluxes of the cleaned membranes ($J_{w,1}$) were measured again. *FRR* is introduced to reflect the resistant fouling ability of the membranes, and higher value of *FRR* means the higher resistant fouling ability. The *FRR* values were calculated and presented in Fig. 6. The *FRR* value is only 61.1% for the reference PI membrane, meaning the existence of serious membrane fouling. The zwitterionic PI membrane has a larger *FRR* value (87.2%), suggesting that the proteins adsorbed and deposited on the membrane surface can be easily washed away. These results are consistent with the protein adsorption experiments. It further confirmed that the zwitterionic groups can prevent direct contact of BSA molecules with the membrane surface, and the protein fouling in the zwitterionic PI membrane was suppressed significantly.

3.2.3 Fouling analysis of the zwitterionic and reference PI membranes

During the ultrafiltration process, the rejected protein molecules adsorbed or deposited on the surface and inside the membrane pores causing membrane fouling, which could be further divided into reversible and irreversible fouling. One part of fouling, recognized as reversible fouling, was caused by reversible protein adsorption or deposition and could be eliminated through hydraulic cleaning (hydrodynamic method); while the other part of fouling, defined as irreversible fouling, could not be eliminated only through hydraulic cleaning. More detailed results of the total fouling ratio (R_t), the reversible fouling ratio (R_r) and the irreversible fouling ratio (R_{ir}) of the two investigated membranes are given in Fig. 6. It can be seen that the R_t value of the reference PI membrane is larger than that of the zwitterionic PI membrane. The bigger R_t value indicates higher total flux loss, corresponding to more protein adsorption and deposition on the membrane surface. Meanwhile, the R_{ir} value of the reference PI membrane is larger among two types of membrane. It can be concluded that the protein fouling on the reference PI membrane is so serious that the fouling can not be removed by hydraulic cleaning. In addition, the zwitterionic PI membrane has not only a lower R_t value but also a lower R_{ir} value, which was already confirmed in protein adsorption experiments. The zwitterionic groups can form strong hydration layer and take up large quantities of free water, which possibly prevents protein molecules from close contact with the membrane surface. These results indicate that the introduction of the zwitterionic units efficiently

reduces total membrane fouling, especially irreversible membrane fouling.

3.2.4 Recycling properties of the zwitterionic and reference PI membranes

In the practical application, the ultrafiltration membrane should keep long-term performance stability and antifouling property which induced a decrease of production cost by decreasing the energy consumption and the cleaning frequencies. A long-term ultrafiltration experiment with three runs was carried out to further investigate the recycling properties of the two investigated membranes, and the results are shown in Fig. 7. After three times of BSA ultrafiltration with a total operation time of 10 h and corresponding three times of hydraulic cleaning, the pure water flux of the reference PI membrane was decreased from 103.8 to 40.2 L/m^{2}h and the flux of BSA solution was only 26.2 L/m^{2}h. However, the pure water flux of the zwitterionic PI membrane can retain at 137.9 L/m^{2}h, the flux of BSA solution could keep at 81.6 L/m^{2}h after three times of BSA solution ultrafiltration. The water flux recovery ratio during each cycle could be calculated to indicate the extent of cleaning efficiency or the effect of irreversible fouling resistance of the membranes, and the results are presented in Fig. 8. For the reference PI membrane, the water flux recovery ratio was 61.1% in the first cycle, and the value increased to 76.9% in the second cycle, and reached 82.3% in the third cycle. It reflects an irreversible fouling was 38.9% in the first cycle, 23.1% in the second cycle, and 17.7% in the third cycle. The amount of newly formed irreversible adsorption of proteins was still significant. For the zwitterionic PI membrane, the water flux recovery ratio was 87.2% in the first cycle, 92.4% in the second cycle, and 96.0% in the third cycle. The degree of irreversible fouling was significantly reduced after each cycle, which ensured high water flux recovery. The excellent performance showed that the zwitterionic PI membrane could be reused for a long time without compromising the water flux. The discussed experimental results suggest that the zwitterionic PI membrane can be a very promising ultrafiltration membrane in the real application.

4. Conclusions

This study is aimed at preparation of the zwitterionic polymer by precise varying the molar ratio of different monomers with specific groups in direct copolymerization method that provides a good opportunity to improve the resultant polymer membrane antifouling performance. The new zwitterionic PI copolymer was successfully synthesized, and the chemical structure was confirmed

by FTIR and ^{1}H NMR measurements. The static water contact angle test showed that some extent of hydrophilic behavior was obtained for the zwitterionic PI membrane. The zwitterionic PI membrane exhibited noticeably larger permeation fluxes during both water and BSA solution filtration than the reference PI membrane. Moreover, the zwitterionic PI membrane has higher flux recovery ratio and lower extent of membrane fouling, especially irreversible membrane fouling, as compared to those of the reference PI membrane, which displayed a unique antifouling performance and longer operation life. In conclusion, the zwitterionic PI has the possibility to be a suitable ultrafiltration membrane material, which is quite beneficial for practical application.

Acknowledgements

This work is financially supported by the Fundamental Research Funds for the Central Universities (No.DL12BB33), the Youths Science Foundation of Heilongjiang Province, China (No.QC2014C044) and the General Financial Grant from the China Postdoctoral Science Foundation (No.2013M530143).

References

[1] M. G. Buonomenna and G. Golemme, in *Advanced materials for membrane preparation,* Bentham Science Publishers Ltd, 2012, Preface.

[2] M. Ulbricht, *Polymer*, 2006, 47, 2217–2262.

[3] N. N. Li, A. G. Fane, W. S. Winston Ho and T. Matsuura, in *Advanced membrane technology and application*, John Wiley & Sons, Inc., 2008, ch. 5, pp. 101−130.

[4] K. Kimura, Y. Hane, Y. Watanabe, G. Amy and N. Ohkuma, *Water Res.*, 2004, 38, 3431−3441.

[5] Y. Liu, S. L. Zhang and G. B. Wang, *Desalination*, 2013, 316, 127−136.

[6] F. M. Jin, W. Lv, C. Zhang, Z. J. Li, R. X. Su, W. Qi, Q. H. Yang and Z. M. He, *RSC Adv.*, 2013, 3, 21394−21397.

[7] R.W. Baker, in *Membrane technology and applications*, John Wiley & Sons, Inc., 3rd edn., 2012, ch. 6, pp. 253−302.

[8] M. Kumar and M. Ulbricht, *RSC adv.*, 2013, 3, 12190–12203.

[9] Y. Liu, X. G. Yue, S. L. Zhang, J. N. Ren, L. L. Yang, Q. H. Wang and G. B. Wang, *Sep. Purif. Technol.*, 2012, 98, 298–307.

[10] D. G. Kim, H. Kang, S. S. Han, H. J. Kim, and J. C. Lee, *RSC adv.*, 2013, 3, 18071–18081.

[11] B. P. Tripathi, N. C. Dubey, F. Simon and M. Stamm, *RSC adv.*, 2014, 4, 6435–6446.

[12] J.N. Ren, Y. Liu, Y. Wang, Q.H. Wang, G.B. Wang, *High Perform. Polym.*, 2013, 25, 714–722.

[13] H. Meng, Q. Cheng and C. X. Li, *Appl. Surf. Sci.*, 2014, 303, 399–405.

[14] A. Laschewsky, *Polymers*, 2014, 6, 1544–1601.

[15] S. F. Chen, S. Y. Jiang, *Adv. Mater.*, 2008, 20, 335–338.

[16] K. Ishihara, H. Nomura, T. Mihara, K. Kurita, Y. Iwasaki and N. Nakabayashi, *J. Biomed. Mater. Res.*, 1998, 39, 323–330.

[17] P. S. Liu, Q. Chen, S. S. Wu, J. Shen and S. C. Lin, *J. Membr. Sci.*, 2010, 350, 387–394.

[18] Q. Shi, Y. L. Su, W. Zhao, C. Li, Y. H. Hu, Z. Y. Jiang and S. P. Zhu, *J. Membr. Sci.*, 2008, 319, 271–278.

[19] Q. F. Zhang, S. B. Zhang, L. Dai and X. S. Chen, *J. Membr. Sci.*, 2010, 349, 217–224.

[20] Y. L. Su and C. Li, *J. Membr. Sci.*, 2008, 68, 161–168.

[21] L. J. Wang, Y. L. Su, L. L. Zheng, W. J. Chen and Z. Y. Jiang, *J. Membr. Sci.*, 2009, 340, 164–170.

[22] C. Liu, L. Li, Z. Liu, M. M. Guo, L. W. Jing, B. J. Liu, Z. H. Jiang, T. Matsumoto and M. D. Guiver, *J. Membr. Sci.*, 2011, 366, 73–81.

[23] S. H. Hsiao, G. S. Liou, Y. C. Kung and H. J. Yen, *Macromolecules*, 2008, 41, 2800–2808.

[24] J. Zhao, Q. Shi, L. G. Yin, S. F. Luan, H. C. Shi, L. Song, J. H. Yin and P. Stagnaro, *Appl. Surf. Sci.*, 2010, 256, 7071–7076.

[25] Y. Wei, H. Q. Chu, B. Z. Dong, X. Li, S. J. Xia and Z. M. Qiang, *Desalination*, 2011, 272, 90–97.

[26] S. Liu, L. Zhou, P. J. Wang, L. S. Zhang, Z. G. Zhao and B. L. Yi, *J. Mater. Chem.*, 2012, 22, 20512–20519.

[27] M. P. Sun, Y. L. Su, C. X. Mu and Z. Y. Jiang, *Ind. Eng. Chem. Res.*, 2010, 49, 790–796.

[28] A. Rahimpour, *Desalination*, 2011, 265, 93–101.

[29] B. Chakrabarty, A. K. Ghoshal and M. K. Purkait, *J. Membr. Sci.*, 2008, 309, 209–221.

[30] Z. Zhang, S. F. Chen, Y. Chang and S. Jiang, *J. Phys. Chem. B*, 2006, 110, 10799–10804.

[31] R. E. Holmlin, X. Chen, R. G. Chapman, S. Takayama and G. M. Whitesides, *Langmuir*, 2001,

17, 2841–2850.

[32] C. Yoshikawa, A. Goto, Y. Tsujii, T. Fukuda, T. Kimura, K. Yamamoto and A. Kishida, *Macromolecules*, 2006, 39, 2284–2290.

Table

Table 1 Summary of properties and performances of the zwitterionic and reference PI membranes.

Membrane	Mean pore size (nm)	Contact angle (º)	Surface energy (mJ/m^2)	Pure water flux (L/m^2h)	Rejection of BSA (%)
Zwitterionic PI	13.7	63.2	45.8	178.3	95.4
Reference PI	10.3	81.7	34.4	103.8	99.5

Scheme Captions

Scheme 1 Synthetic route for diamine monomer TPA-NMe_2.

Scheme 2 Synthetic route for diamine monomer BAPBS.

Figure Captions

Fig. 1 Schematic illustration of the procedure for the preparation of the zwitterionic PI copolymer and the zwitterionic PI membrane.

Fig. 2 SEM images of the cross-section (1) and surface (2) of the zwitterionic (a) and reference (b) PI membranes. EDX S-mapping on the surface of the zwitterionic (a3) and reference (b3) PI membranes (magnification: 40×).

Fig. 3 Contact angle images of the zwitterionic (a) and reference (b) PI membranes.

Fig. 4 Protein adsorption on the zwitterionic (green) and reference (white) PI membranes.

Fig. 5 Time-dependent fluxes of the zwitterionic and reference PI membranes during the protein ultrafiltration experiment.

Fig. 6 Summary of the flux recovery ratio (*FRR*), the total fouling ratio (R_t), the reversible fouling ratio (R_r) and the irreversible fouling ratio (R_{ir}) of the zwitterionic and reference PI membranes during the protein ultrafiltration experiment.

Fig. 7 Time-dependent recycling fluxes of the zwitterionic and reference PI membranes during three cycles of the protein ultrafiltration experiment.

Fig. 8 The flux recovery ratio (*FRR*) of the zwitterionic and reference PI membranes after various cycles of the protein ultrafiltration experiment.

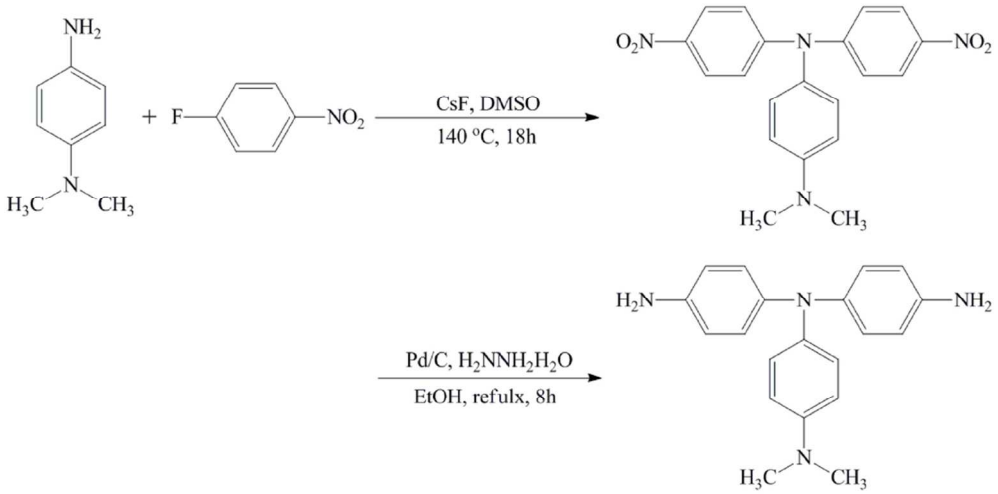

Scheme 1 Synthetic route for diamine monomer TPA-NMe_2.
49x24mm (600 x 600 DPI)

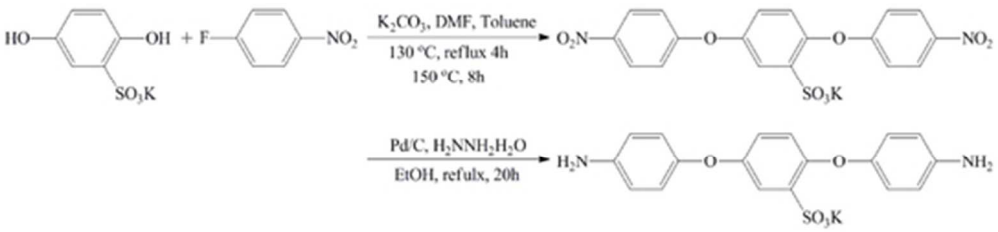

Scheme 2 Synthetic route for diamine monomer BAPBS.
23x5mm (600 x 600 DPI)

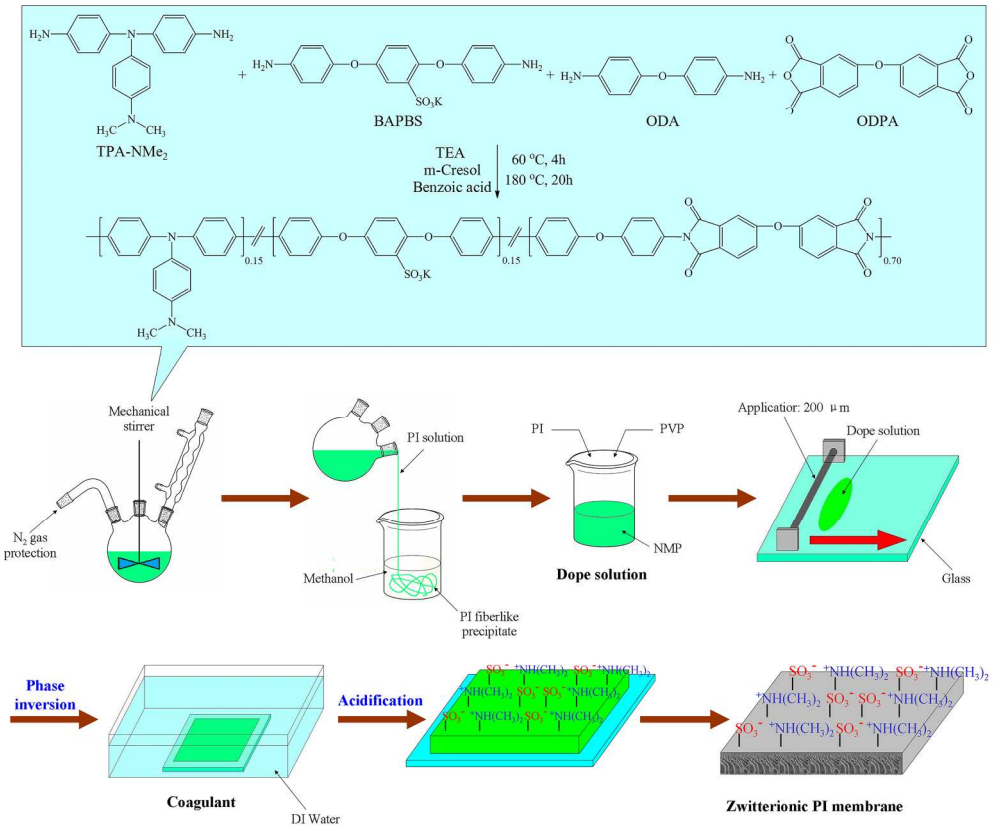

Fig. 1 Schematic illustration of the procedure for the preparation of the zwitterionic PI copolymer and the zwitterionic PI membrane.
98x81mm (600 x 600 DPI)

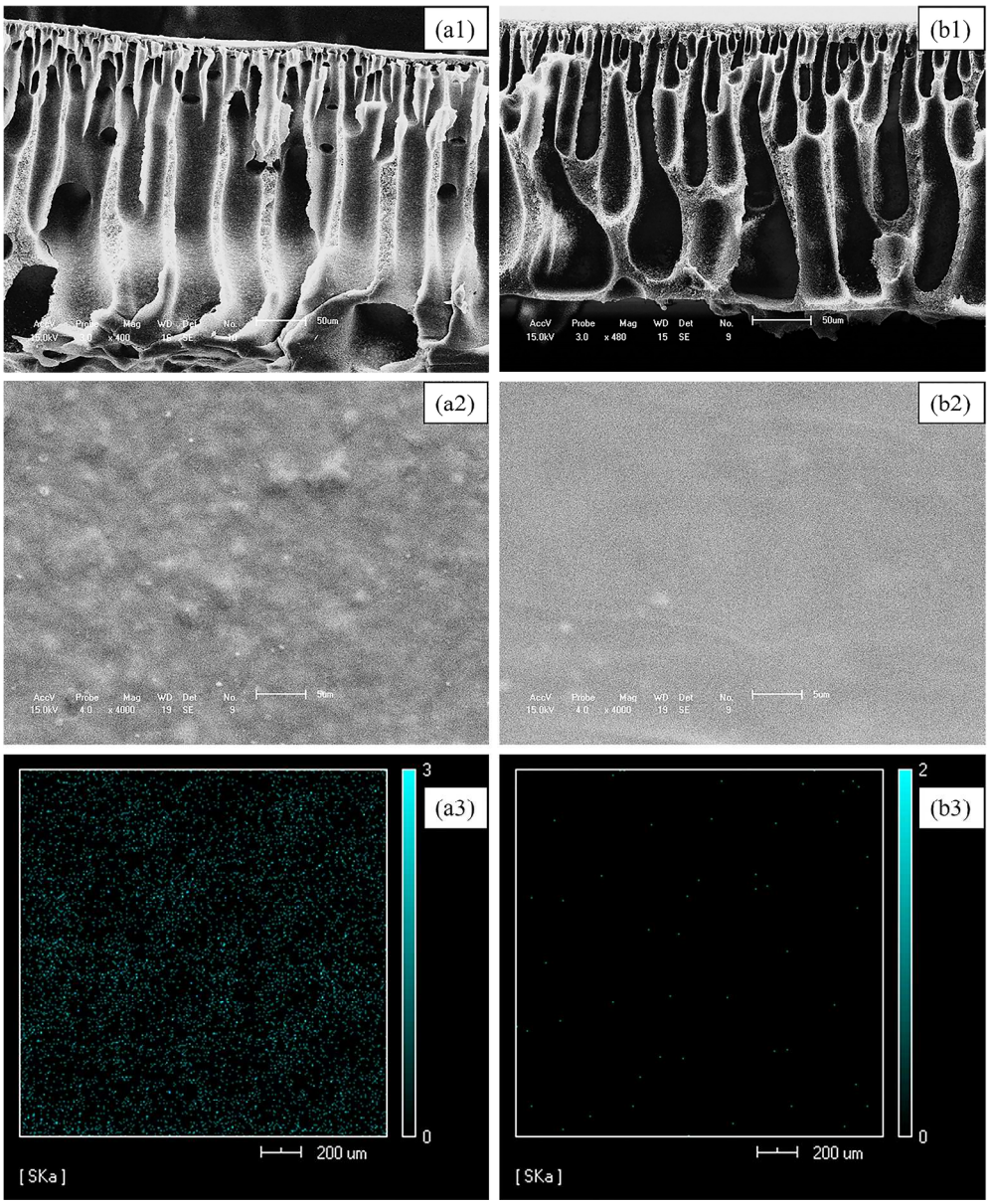

Fig. 2 SEM images of the cross-section (1) and surface (2) of the zwitterionic (a) and reference (b) PI membranes. EDX S-mapping on the surface of the zwitterionic (a3) and reference (b3) PI membranes (magnification: 40×).
97x117mm (600 x 600 DPI)

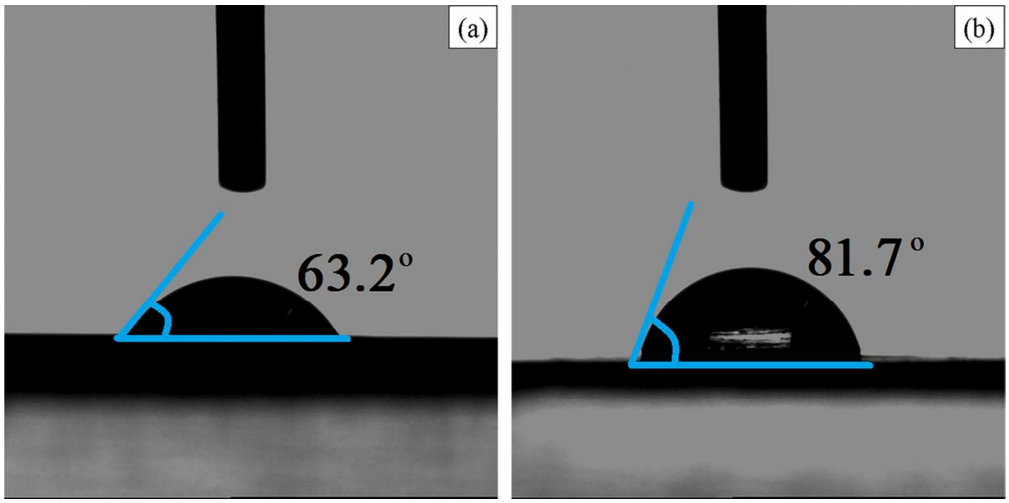

Fig. 3 Contact angle images of the zwitterionic (a) and reference (b) PI membranes.
59x29mm (600 x 600 DPI)

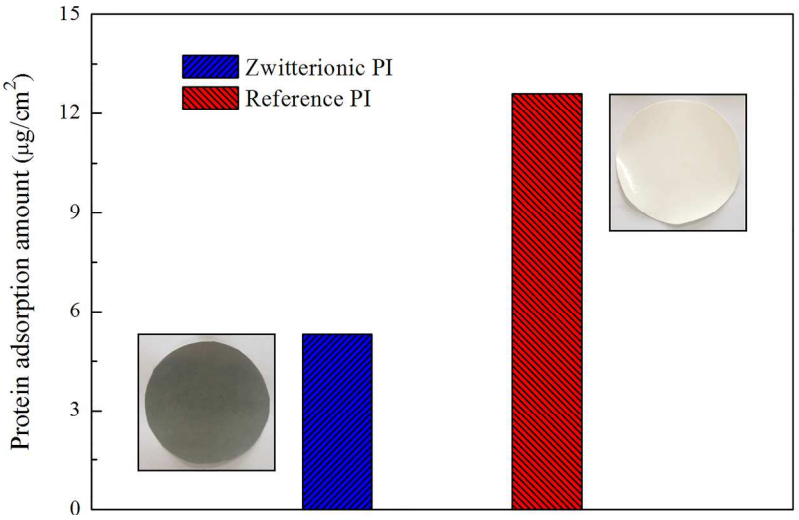

Fig. 4 Protein adsorption on the zwitterionic (green) and reference (white) PI membranes.
99x70mm (600 x 600 DPI)

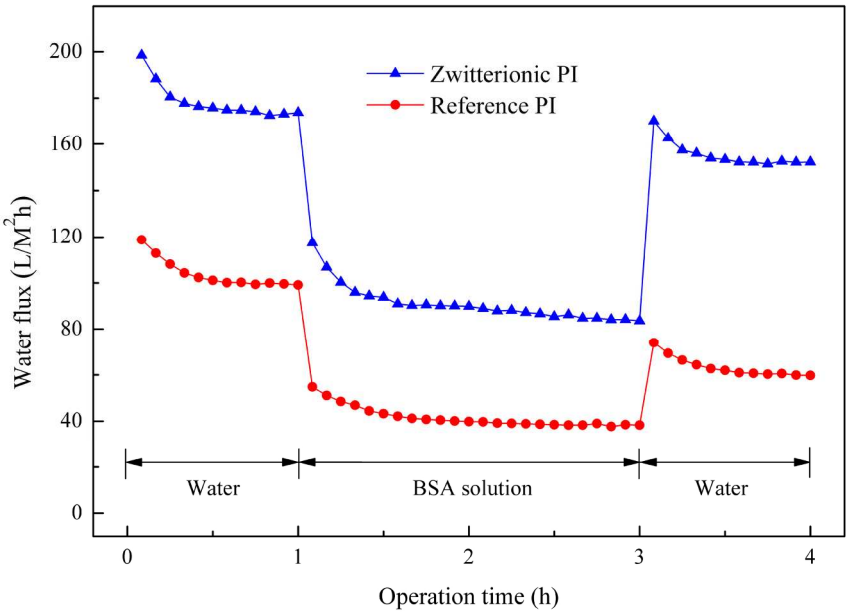

Fig. 5 Time-dependent fluxes of the zwitterionic and reference PI membranes during the protein ultrafiltration experiment.
99x70mm (600 x 600 DPI)

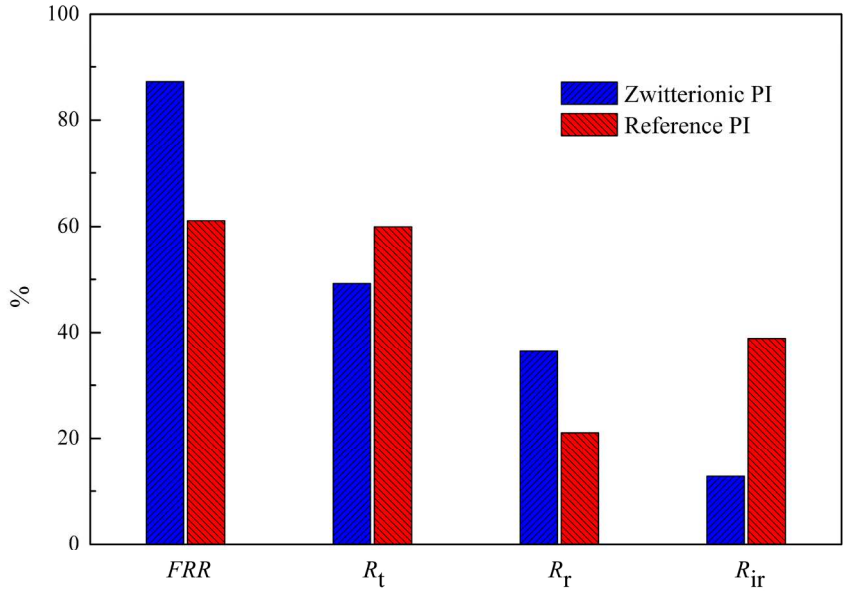

Fig. 6 Summary of the flux recovery ratio (*FRR*), the total fouling ratio (R_t), the reversible fouling ratio (R_r) and the irreversible fouling ratio (R_{ir}) of the zwitterionic and reference PI membranes during the protein ultrafiltration experiment.
99x70mm (600 x 600 DPI)

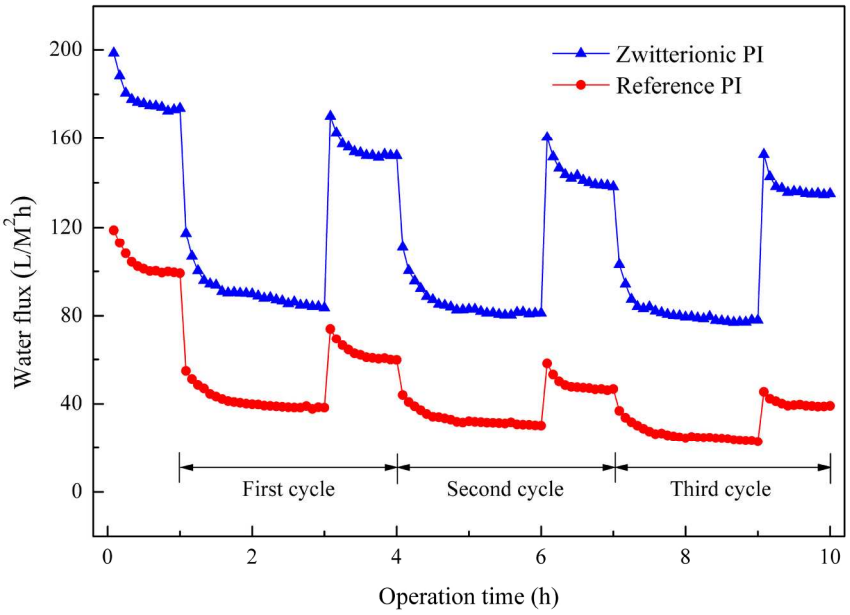

Fig. 7 Time-dependent recycling fluxes of the zwitterionic and reference PI membranes during three cycles of the protein ultrafiltration experiment.
99x70mm (600 x 600 DPI)

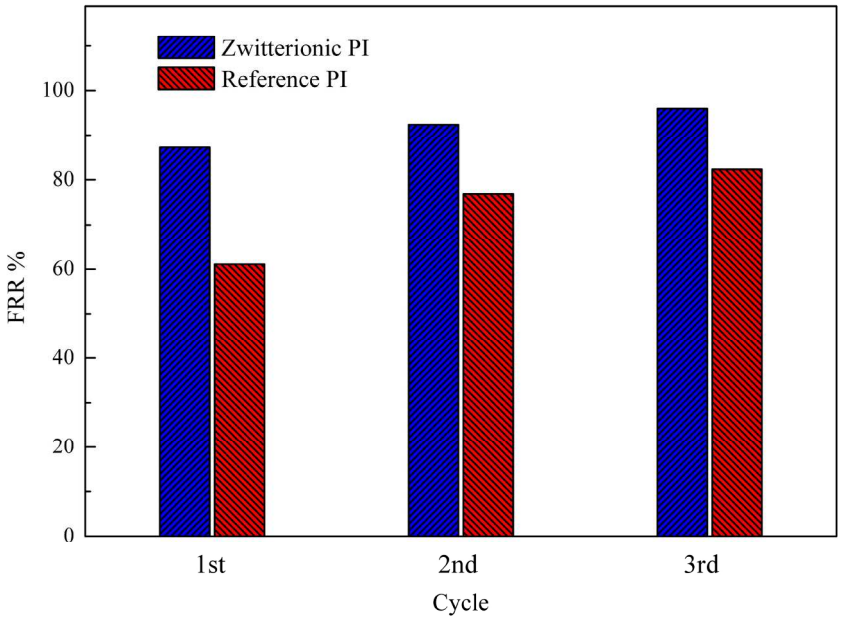

Fig. 8 The flux recovery ratio (FRR) of the zwitterionic and reference PI membranes after various cycles of the protein ultrafiltration experiment.
99x70mm (600 x 600 DPI)